ELSEVIER

Bone 36 (2005) 489–501

BONE

www.elsevier.com/locate/bone

Effects of hyaluronan on three-dimensional microarchitecture of subchondral bone tissues in guinea pig primary osteoarthrosis

Ming Ding[a,b,*], Carl Christian Danielsen[c], Ivan Hvid[a,d]

[a]*Orthopaedic Research Laboratory, Department of Orthopaedics, Aarhus University Hospital, Aarhus, Denmark*
[b]*Orthopaedic Research Laboratory, Department of Orthopaedics and Laboratory for Molecular Endocrinology, Odense University Hospital, Odense, Denmark*
[c]*Department of Connective Tissue Biology, Institute of Anatomy, University of Aarhus, Aarhus, Denmark*
[d]*Department of Orthopaedics, Aalborg University Hospital, Aalborg, Denmark*

Received 2 September 2004; revised 3 November 2004; accepted 1 December 2004

Abstract

Hyaluronan (HA) has received increasing interest as a potential agent in therapeutic intervention in osteoarthrosis (OA). HA has been shown to reduce arthritic lesions in experimental animal models of articular cartilage injury. This study was to investigate the effects of high molecular weight HA intra-articular injection on subchondral bone tissues.

Fifty-six male guinea pigs were randomly divided into 5 groups. During the initial 2.5-month period, three groups received intra-articular injection of HA 0.4 mg/kg/week for 5 weeks in both knee joints. Two control groups received vehicle. After 2.5 months, one HA group and one control group were sacrificed. The remaining 3 groups (5.5-month groups) were left for an additional 3 months before sacrifice during which time one HA group received additional 5 weeks injections, one HA group received no more injections, and the control group received vehicle. The left tibiae were harvested and micro-CT scanned to quantify three-dimensional microarchitecture of subchondral bone plate, cancellous bone and cortical bone, followed by mechanical testing and collagen and mineral determinations.

All HA-treated groups had almost normal cartilage, whereas the control groups had typical OA-related cartilage degradation. In the 2.5-month group, HA resulted in significantly decreased subchondral plate volume fraction and thickness and HA-treated cancellous bone had significantly lower bone volume fraction, and typical rod-like structure. After 5.5 months, these changes were more pronounced, with an additional marked decrease in connectivity and bone surface density. HA-treated cortical bone had significantly greater volume fraction at both observation times. HA groups had greater bone mineral concentration and reduced collagen to mineral ratio with similar mechanical properties of cancellous bone but less stiff cortical bone. The effects of HA on cartilage and subchondral bone were maintained when treatment was discontinued.

In summary, HA effectively protects against cartilage degeneration, decreases subchondral bone density and thickness, changes trabecular structure toward rod-like, so that subchondral bone becomes more compliant and thereby reduces cartilage stress during impact loading. HA preserved cancellous bone mechanical properties by increasing bone mineralization. Early HA administration is effective for intervention of OA initiation and progression, and short-term early HA treatment is sufficient to maintain treatment effects.

Keywords: Hyaluronan; Primary guinea pig osteoarthrosis; Three-dimensional microarchitecture; Mechanical properties; Bone collagen and mineral

Introduction

Hyaluronan (HA) is a biologic material, and a major component of synovial fluid. HA plays a central role in joint cavity formation during development. Currently, HA has received increasing interest as a potential agent of therapeutic intervention in osteoarthrosis (OA) [27,28]. High

* Corresponding author. Department of Orthopaedics O, Odense University Hospital, Sdr. Boulevard 29, DK-5000 Odense, Denmark. Fax: +45 6614 2145.
E-mail addresses: ming.ding@ouh.fyns-amt.dk, m_ding_dk@hotmail.com (M. Ding).

8756-3282/$ - see front matter © 2004 Elsevier Inc. All rights reserved.
doi:10.1016/j.bone.2004.12.010

molecular weight HA has been applied to the clinical therapy of human OA and experimental OA. Investigations have shown that intra-articular injection of HA reduces arthritic lesions in experimental animal models of articular cartilage injury [1,26]. It has been observed that intra-articular injections of HA effectively coat the articular surface of intact cartilage. In disrupted cartilage surfaces, HA results in deeper penetration of HA into the crevice formed by the cartilage fibrillation and deeper penetration into the cartilage matrix. The observed HA-covering of articular surface suggests that the major beneficial effect of HA is an enhanced anabolism, more than a physical one [28]. Nevertheless, it has not been fully elucidated how HA affects underlying subchondral bone tissue. It is unclear whether HA has any effect on the underlying subchondral bone tissues, e.g. three-dimensional (3-D) microarchitecture, density, collagen and mineral.

OA is a degenerative joint disease that has been characterized by progressive articular cartilage damage and by sclerosis and hypomineralization of the underlying subchondral bone tissues beneath the joint surface. Both cartilage and subchondral cancellous bone may play significant roles. Male Dunkin–Hartley guinea pigs Charles River strain displays a spontaneous onset of progressive degenerative changes in the knee joint similar to human OA [2]. The earliest histological signs of OA appeared at the 3 months of age in the medial compartment and progressed to moderate or severe degenerative changes at 12 months of age [2,3,8,19]. Some investigations have been carried out that focus on articular cartilage and subchondral bony changes in this OA model.

Recent investigations have demonstrated that subchondral bone plate and cancellous bone are involved in the pathogenesis of OA [7,9,14]. It is still a matter of debate whether subchondral bone changes in OA are preceding, concurring with or following cartilage degeneration. There are two opposing hypotheses: bone sclerosis is secondary to cartilage loss and the result of cartilage breakdown; bone sclerosis precedes cartilage degeneration and loss—the Radin hypothesis [25].

Previous investigations have revealed reduced mechanical properties of early-stage human OA subchondral cancellous bone. This reduction seems due to a decreasing bone quality that could not fully be compensated for by the increasing bone mass of inferior mechanical quality [11]. In severe OA, the increased total amount of cancellous bone tissue did not proportionally relate to either the increased mechanical properties [21], or the unchanged mechanical properties between OA and normal controls [5]. The lack of relation may be due to undermineralization of bone in OA [5]. It is thus postulated that bone quality deteriorates in OA cancellous bone tissues. The changes in the density and microarchitecture of the underlying subchondral bone have a profound effect on the initiation and progression of articular cartilage degeneration [25].

Our recent investigation using a primary guinea pig OA has demonstrated that different mechanisms exist in the subchondral bone plate, cancellous bone and cortical shell [9]. Significant changes in subchondral bone collagen and mineral have been observed, particularly at the medial condyle of severe stage OA. Increased collagen to mineral ratio, reflecting the degree of mineralization, suggests abnormal bone collagen and mineral metabolisms in severe OA [24], since the degree of bone mineralization influences its biomechanical competence [4]. It would be of particular interest to investigate whether application of HA has any effect on the 3-D microarchitecture, mechanical properties and bone collagen content and mineralization of underlying subchondral bone tissues.

The aims of the current study were to investigate the effects of high molecular weight HA (1.5×10^6 Da) intra-articular injection on the microarchitecture, mechanical properties, collagen and mineral of subchondral bone tissues. We tested the hypothesis that HA protects against cartilage degeneration, decreases subchondral bone density and changes its 3-D microarchitecture so that subchondral bone becomes more compliant and thereby reduces cartilage stress during impact loading. We examined the effects of 5 weeks of HA administration on subchondral bone tissues, whether continuous HA administration for an additional 5 week period would increase the effects of HA on bone, and whether the effects could be maintained once HA was discontinued.

Materials and methods

Experimental animals

Fifty-six male Charles River strain outbred Dunkin–Hartley guinea pigs were used in this study (HB Lidköpings Kaninfarm, Lidköping, Sweden). These guinea pigs were acclimated for a period of 2 months before initiation of the study. The guinea pigs were housed 2–3 in the environmentally controlled cage and fed standard guinea pig chow that contained 18% protein, 0.9% calcium, 0.7% phosphorus and 600 IU/kg vitamin D3 (Altromin Standard Guinea Pig Chow #3020, Lage, Germany). Food and water were ad libitum. The guinea pigs were 6 months of age at the beginning of the study. The experimental procedures were in accordance with Danish Animal Research guidelines, and the research protocol was approved by the Danish Animal Experiment Committee (Study no. J.nr. 2000/561-329).

Experimental design

The guinea pigs were randomly divided into 5 groups (Table 1) based on their ages and body weight (n is given in Table 1). Physical well-being and activity were checked daily, and body weight was measured weekly. The weights of each animal were recorded at the start and at the end of

Table 1
Experimental design

Groups	N	Day of treatment (age, in months)											
		1 (6.5)	8	15	22	29	75 (9)	90 (9.5)	97	104	111	118	165 (12)
2.5-month experimental period													
G1: HA HA for 5 weeks	10	●	●	●	●	●	Sacrifice						
G2: control 2.5 saline for 5 weeks	10	○	○	○	○	○	Sacrifice						
5.5-month experimental period													
G3: HA repetition HA for 5 weeks, and repeated for 5 weeks	12	●	●	●	●	●		●	●	●	●	●	Sacrifice
G4: HA discontinuation HA for 5 weeks, then discontinued HA	12	●	●	●	●	●							Sacrifice
G5: control 5.5 saline for 5 weeks, then repeated for 5 weeks	12	○	○	○	○	○		○	○	○	○	○	Sacrifice

● Hyaluronan intra-articular injection 0.4 mg/kg/week.
○ Physiological saline intra-articular injection 0.1 ml saline.

the experiment. The treatments started in all groups when the guinea pigs were 6.5 months old. Three groups received intra-articular injections in both knees of HA 0.4 mg/kg/week and two groups received vehicle (0.1 ml saline/week) for 5 weeks. Thereafter, the guinea pigs were left untreated until they were 9 months old. At this age, two groups (2.5-month groups), an HA group and a saline group, were sacrificed. For the remaining three groups, 2 groups received once more the same treatment regimen (HA or saline injections for 5 weeks as before) starting when the guinea pigs were 9.5 months old, and one HA group was left untreated. The latter 3 groups (5.5-month groups) were sacrificed when the guinea pigs were 12 months old (Table 1).

Before injection, the guinea pig received pre-medication with atropine sulfate 0.004 mg/kg, and sedation with sodium stesolid (Diazepam) 5 mm/kg (Sigma-Aldrich Denmark A/S, Copenhagen, Denmark). Thereafter, both knees were washed with 70% alcohol. Intra-articular injections were performed under aseptic conditions using 26 gauge, 1/2 in. 0.45 × 12 needle (Terumo Corperatio, Leuven, Belgium) on a tuberculin syringe to insert beneath the patella in the region of the pattellofemoral joint and 0.1 ml HA or vehicle was injected. All the injections were performed by the same person (MD). Sodium hyaluronate was purchased from Lifecore Biomedical, Inc. (Chaska, MN 55318 USA). The molecular weight was approximately 1.5×10^6 Da. Sodium hyaluronate was dissolved in physical saline before injection and 1 ml contained 4 mg hyaluronate. Animals tolerated well the injection procedure without any adverse reaction, and they were placed in their cages to recover from the anesthesia. At the completion of the experiment, the guinea pigs were killed and left tibiae of the guinea pigs were dissected and kept in sealed plastic bags at −20°C.

Grading degree of osteoarthrosis

After micro-CT scanning, the sectioned articular cartilage and subchondral plate complex was embedded in methylmethacrylate (MMA) and three slices (8 μm) from each medial condyle and lateral condyle were sectioned using an universal heavy-duty microtome (Reichert-Jung, Cambridge Instruments GmbH, Germany). These cartilage sections were stained with Safranin O. The degree of cartilage degeneration was defined and graded according to Mankin's criteria [23] (Table 2).

Table 2
Guinea pig body weight and Mankin's score [mean (95% confidence interval)]

Groups	2.5-month experimental period			5.5-month experimental period			One-way ANOVA for G3 to G5	One-way ANOVA for all HA groups
	G1: HA	G2: control 2.5	*t* test for G1 and G2	G3: HA-repetition	G4: HA-discontinuation	G5: control 5.5		
Body weight at start (g)	1027 (984–1070)	1024 (977–1071)	$P = 0.92$	1049 (992–1106)	983 (933–1034)	1030 (990–1070)	$P = 0.28$	$P = 0.18$
Body weight at sacrifice (g)	1125 (1077–1173)	1115 (1047–1182)	$P = 0.80$	1183 (1102–1264)	1162 (1093–1232)	1119 (1035–1203)	$P = 0.49$	$P = 0.47$
Mankin's score for medial tibial cartilage	1.3 (0.52–2.08)	4.5 (2.87–6.13)	$P = 0.004$	1.69 (0.50–2.89)	1.80 (0.64–2.96)	7.14 (6.18–9.07)	$P < 0.001$, G5 > G3, G4	$P = 0.79$
Mankin's score for lateral tibial cartilage	1.40 (0.51–2.29)	3.90 (2.29–5.51)	$P = 0.02$	1.50 (0.66–2.34)	1.03 (0.19–1.88)	5.27 (3.52–7.02)	$P < 0.001$, G5 > G3, G4	$P = 0.75$

Micro-computerized tomography (micro-CT)

The proximal tibiae of the guinea pigs were micro-CT scanned using a high resolution micro-CT system (μCT 40, Scanco Medical AG., Zürich, Switzerland). The first scan was made on proximal tibia for quantifying the micro-architecture of subchondral bone plate. After the first scan, proximal tibia was cut 0.5 mm beneath subchondral plate and a further cut was made distally to produce 3 mm thick cancellous–cortical bone specimen using a LEITZ Microtome 1600 (Ernst Leitz Wetzlar Gmbh, Wetzlar, Germany). The second scan was made on this cortical–cancellous bone complex for quantifying microarchitecture of subchondral cancellous bone and cortical bone. These scanned images had an isotropy spatial resolution of 19 μm^3. The three-dimensional (3-D) reconstruction cubic voxel sizes were 16 * 16 * 16 μm^3 (1024 × 1024 pixels) with 16-bit-gray-levels. Micro-CT images were segmented using previously described segmentation techniques [13] with some modification [9] to acquire accurate 3-D imaging datasets for the subchondral bone plate, cancellous bone and cortical bone.

Three-dimensional microarchitectural properties of subchondral bone plate

According to definition, subchondral plate was defined as starting from the calcified cartilage-bone junction and ending at the marrow space (Fig. 1) [7]. The meaningful microarchitectural parameters for the subchondral bone plate were determined. Plate volume fraction (bone volume per total plate volume, %), plate thickness (μm), surface density (plate surface to total plate volume, mm^{-1}) and mean plate perforation (μm) were calculated. These calculations were done first on total subchondral plate, then on the medial and lateral condyles (Fig. 1).

Three-dimensional microarchitectural properties of subchondral cancellous bone

Subchondral cancellous bone was defined as the epiphyseal cancellous bone region 0.5 mm beneath subchondral plate. 3-D micro-CT imaging data of cancellous bone were segmented and separated from the cortical shell (Fig. 2). The microstructural properties were calculated using true, unbiased and assumption-free 3-D methods. Specifically, bone volume fraction [13] and trabecular thickness (μm) [17] were determined. Structure model index (SMI) was based on a differential analysis of the triangulated bone surface of a structure. The quantification of architectural anisotropy was based on the mean intercept length method. The degree of anisotropy was defined as the ratio between primary and tertiary eigenvalues. Connectivity density, the number of multiple connected trabeculae per volume (mm^{-3}), was based on a topological approach. Bone surface density (mm^{-1}) and trabecular spacing (μm) were also calculated (Fig. 2).

Three-dimensional microarchitectural properties of subchondral cortical bone

Subchondral cortical bone was defined as the epiphyseal cortical bone region 0.5 mm beneath subchondral plate and 3 mm distal. 3-D imaging data of cortical bone were segmented and separated from the cancellous bone (Fig. 2). Bone volume fraction (%) [13], cortical thickness (μm), bone surface density (mm^{-1}) [17], and cortical bone porosity (cavity/perforation, %) were calculated. The cross sectional area (mm^2) of cortical bone was the mean value obtained from the subchondral cortical bone (Fig. 2).

Compression testing of proximal tibial metaphysis

Mechanical tests of 3 mm high proximal tibia bone specimens (cancellous–cortical complex) were performed on an 858 Bionix MTS hydraulic material testing machine (MTS Systems Co., Minneapolis, Minnesota, USA), using a 1 kN load cell. After 10 preconditioning cycles, the mechanical testing of proximal cortex was first performed using a technique ("reduced platen testing") in which the central cancellous bone was compressed by 10% in the axial loading direction only, thus keeping the cortex and the remaining peripheral cancellous bone intact [18]. Compression test to failure was subsequently performed on the cortical shell (mainly cortical bone but including a brim of cancellous bone) [9].

For cancellous bone, maximal load of mechanical testing was recorded. Young's modulus was calculated as the tangent to the linear portion of the stress–strain curve between 0.4% and 0.6% stain. Ultimate stress (strength) was defined as the first point with maximal stress, and the corresponding ultimate strain was calculated. Failure energy was calculated as the area underneath the compression curve between zero strain and ultimate strain. For cortical bone, the same mechanical parameters were calculated [10]. The cross sectional area of the remaining cortical specimen was calculated as the mean cross sectional area of both proximal and distal ends of the specimen (measured from micro-CT images) minus the contact areas of testing columns for the reduced platen test [9].

Determination of bone density, collagen and mineral

After mechanical testing, the 3 mm specimen was defatted. Dry weight was measured and submerged weight of specimens was determined (Mettler AT250 balance, Mettler Instruments AG, Greifensee, Switzerland) using Archimedes' principle [10]. Due to the irregular shape of specimens, total bone volumes were determined

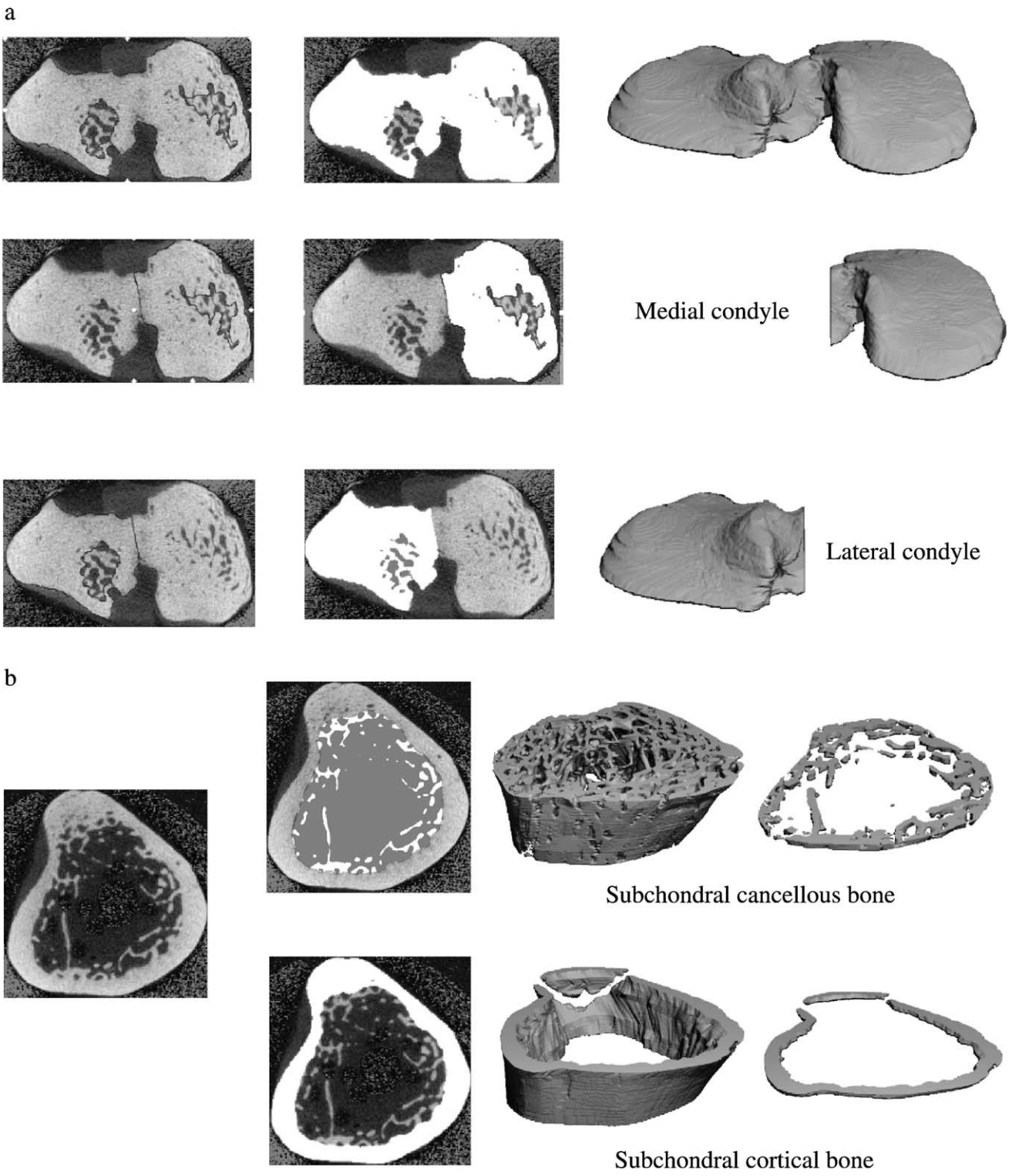

Fig. 1. (a) Project protocol for micro-CT scanning and microarchitectural analysis of guinea pig proximal tibia. Proximal tibiae were micro-CT scanned. From 2-D micro-CT images (left), 3-D reconstruction (right) and microarchitectural analysis were performed first on overall subchondral plate, then on the medial and lateral condyles. (b) After first scanning, a 3 mm thick bone specimen was sawed out 0.5 mm beneath subchondral plate. A second scanning was done on this specimen. From 2-D micro-CT images (left), a specific contouring was made that separated cortical bone from cancellous bone. 3-D imaging datasets of cancellous and cortical bone were separately reconstructed (right) and microarchitectural analyses of cancellous and cortical bone were performed on overall as well as on the medial and the lateral condyles.

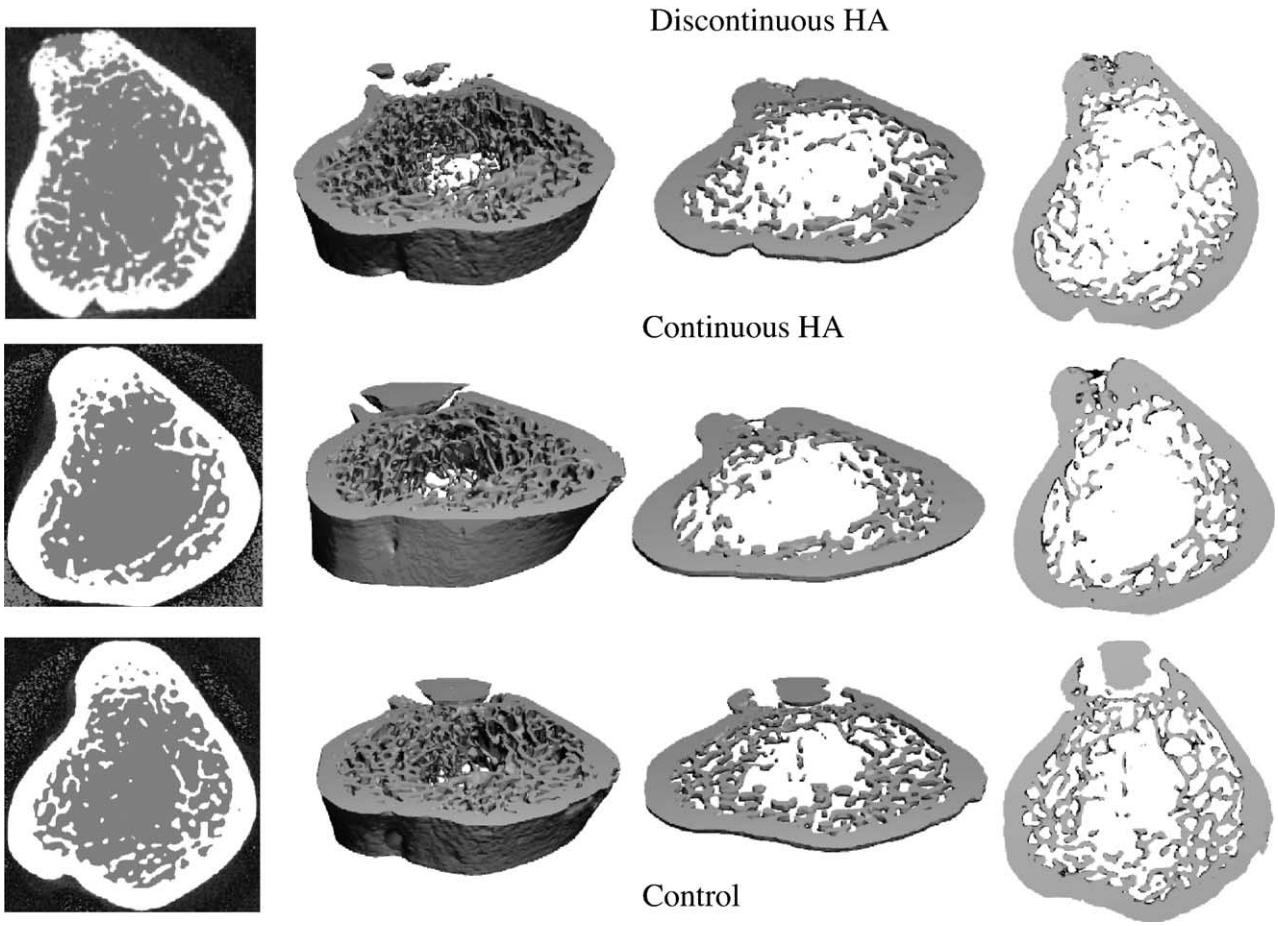

Fig. 2. Examples of 3-D reconstruction of micro-CT imaging for the HA discontinuation, the HA repetition and the control 5.5-month experimental groups. Marked differences in the microarchitecture of subchondral bone are seen. Samples represent the median values of the bone volume fraction.

from micro-CT images. Tissue density and apparent density of the specimens were calculated [10]. Then, the specimens were sectioned into two parts—medial and lateral condyle sub-specimens. Two pieces from each condyle were used for determinations of collagen, mineral and densities according to a previously described procedure [10].

Statistical analysis

All statistical analyses were performed using SPSS software version 10.0.7 (SPSS Inc. Chicago, Illinois, USA). Normality and equal variance of the data were checked. Two sample *t* tests were done to examine differences in properties between the 2.5-month HA and the control groups. One-way analyses of variance (ANOVA) were performed followed by post hoc Bonferroni or Dunnett's corrected *t* tests to determine which specific differences were significant in the three 5.5-month groups. ANOVA was also used to examine if there was significant difference among all three HA groups. A P value <0.05 was considered significant.

Results

The different treatments did not influence the body weight (Table 2) or the weight gain (not shown) of the guinea pigs. The Mankin's scores for the medial and lateral condyles are summarized in Table 2. Progressive cartilage degenerations are seen in both condyles of 9 and 12 months control groups and the degeneration was particularly pronounced in the medial condyle. Chondrocyte death and proteoglycan loss with cartilage fibrillation were seen on the medial tibial plateau in both age groups. Incidence and severity of the cartilage lesions increased with age, and by 12 months of age, all animals in the control group had moderate degeneration of the medial tibial plateau. In contrast, all the HA-treated groups after both experimental periods had only slight articular cartilage fibrillation in the medial condyles, and the lateral condyles were almost normal.

Descriptive statistical analysis of the 3-D microarchitectural properties of the subchondral bone plate (Table 3), cancellous bone (Table 4), cortical bone (Table 5), bone collagen and mineral (Table 6) and the mechanical proper-

Table 3
Three-dimensional microarchitectural properties [mean (95% confidence interval)] of subchondral bone plate (total, medial and lateral)

Groups	2.5-month experimental period			5.5-month experimental period				
	G1: HA	G2: control 2.5	*t* test for G1 and G2	G3: HA-repetition	G4: HA-discontinuation	G5: control 5.5	One-way ANOVA for G3 to G5	One-way ANOVA for all HA groups
Plate volume fraction (%)								
Total	97.8 (96.5–99.1)	99.9 (99.8–1.00)	$P < 0.001$	99.9 (99.5–1.00)	99.9 (99.7–1.00)	99.8 (97.9–1.00)	$P = 0.89$	$P = 0.002$, G1 < G3, G4
Medial	98.2 (97.3–99.2)	99.9 (99.7–1.00)	$P < 0.001$	99.9 (99.6–1.00)	99.9 (99.8–1.00)	99.9 (99.6–1.00)	$P = 0.91$	$P = 0.001$, G1 < G3, G4
Lateral	97.4 (95.4–99.5)	99.4 (98.5–1.00)	$P = 0.10$	99.0 (98.6–1.00)	99.6 (99.0–1.00)	98.7 (96.0–1.00)	$P = 0.92$	$P = 0.06$
Paired *t* test medial vs. lateral	$P = 0.43$	$P = 0.011$		$P = 0.023$	$P = 0.023$	$P = 0.30$		
Plate thickness (μm)								
Total	349 (322–377)	365 (343–386)	$P = 0.40$	380 (360–400)	381 (361–402)	357 (335–379)	$P = 0.20$	$P = 0.10$
Medial	319 (299–338)	373 (346–400)	$P = 0.01$	375 (347–404)	396 (373–419)	374 (351–398)	$P = 0.47$	$P = 0.001$, G1 < G3, G4
Lateral	380 (340–419)	356 (338–375)	$P = 0.30$	384 (371–397)	367 (343–391)	340 (312–368)	$P = 0.09$	$P = 0.68$
Paired t test medial vs. lateral	$P < 0.001$	$P = 0.06$		$P = 0.48$	$P = 0.024$	$P = 0.042$		
Plate surface density (mm^{-1})								
Total	3.64 (3.35–3.92)	4.01 (3.79–4.23)	$P = 0.054$	3.82 (3.68–3.97)	4.05 (3.72–4.39)	4.03 (3.21–4.85)	$P = 0.82$	$P = 0.11$
Medial	3.79 (3.45–4.12)	4.13 (3.87–4.94)	$P = 0.07$	4.10 (3.85–4.36)	4.11 (3.77–4.45)	4.23 (3.33–5.12)	$P = 0.84$	$P = 0.29$
Lateral	3.58 (3.27–3.90)	3.81 (3.56–4.07)	$P = 0.27$	3.72 (3.55–3.90)	4.04 (3.68–4.40)	3.99 (2.96–5.02)	$P = 0.65$	$P = 0.10$
Paired *t* test medial vs. lateral	$P = 0.15$	$P = 0.09$		$P = 0.07$	$P = 0.59$	$P = 0.74$		
Plate perforation (μm)								
Total	86 (70–101)	70 (63–77)	$P = 0.09$	73 (62–85)	77 (70–84)	77 (68–85)	$P = 0.86$	$P = 0.36$
Medial	84 (66–101)	68 (60–75)	$P = 0.11$	77 (56–99)	70 (63–76)	69 (59–80)	$P = 0.49$	$P = 0.40$
Lateral	87 (64–111)	72 (64–81)	$P = 0.25$	70 (55–85)	84 (75–93)	84 (71–97)	$P = 0.13$	$P = 0.36$
Paired *t* test medial vs. lateral	$P = 0.65$	$P = 9.23$		$P = 0.66$	$P = 0.004$	$P = 0.11$		

Table 4
Three-dimensional microarchitectural properties [mean (95% confidence interval)] of subchondral cancellous bone

Groups	2.5-month experimental period			5.5-month experimental period				
	G1: HA	G2: control 2.5	*t* test for G1 and G2	G3: HA-repetition	G4: HA-discontinuation	G5: control 5.5	One-way ANOVA for G3 to G5	One-way ANOVA for all HA groups
Bone volume fraction (%)	29.3 (27.1–31.6)	35.6 (31.8–39.5)	$P = 0.020$	31.7 (29.1–34.3)	30.5 (26.8–34.2)	38.8 (36.3–41.4)	$P = 0.001$, G5 > G3, G4	$P = 0.50$
Trabecular thickness (μm)	121 (114–128)	128 (120–136)	$P = 0.136$	129 (124–134)	127 (118–135)	131 (126–135)	$P = 0.66$	$P = 0.21$
Structure model index (–)	1.58 (1.41–1.76)	0.94 (0.68–1.19)	$P = 0.003$	1.18 (1.00–1.35)	1.23 (1.02–1.45)	0.58 (0.31–0.84)	$P = 0.001$, G5 > G3, G4	$P = 0.007$, G1 > G3, G4
Architecture anisotropy (–)	1.35 (1.30–1.41)	1.32 (1.28–1.36)	$P = 0.785$	1.41 (1.38–1.44)	1.38 (1.25–1.52)	1.30 (1.22–1.39)	$P = 0.23$	$P = 0.60$
Connectivity density (mm^{-3})	41.5 (36.6–46.5)	50.8 (42.2–59.5)	$P = 0.171$	35.3 (31.2–39.5)	34.0 (30.0–38.0)	46.1 (43.5–48.6)	$P = 0.001$, G5 > G3, G4	$P = 0.04$
Bone surface density (mm^{-1})	6.10 (5.77–6.44)	6.69 (6.16–7.23)	$P = 0.149$	5.96 (5.58–6.33)	5.82 (5.39–6.24)	6.78 (6.57–7.00)	$P = 0.001$, G5 > G3, G4	$P = 0.56$
Trabecular spacing (μm)	314 (281–347)	292 (253–332)	$P = 0.247$	349 (312–386)	353 (307–399)	274 (255–292)	$P = 0.006$, G5 < G3, G4	$P = 0.31$

Table 5
Three-dimensional microarchitectural properties [mean (95% confidence interval)] of subchondral cortical bones

Groups	2.5-month experimental period			5.5-month experimental period				
	G1: HA	G2: control 2.5	*t* test for G1 and G2	G3: HA-repetition	G4: HA-discontinuation	G5: control 5.5	One-way ANOVA for G3 to G5	One-way ANOVA for all HA groups
Bone volume fraction (%)	99.5 (98.9–1.00)	95.8 (94.9–96.7)	$P < 0.001$	99.5 (98.8–1.00)	99.6 (98.9–1.00)	94.7 (93.7–95.7)	$P < 0.001$, G5 < G3, G4	$P = 0.98$
Cortical thickness (μm)	400 (377–423)	376 (339–412)	$P = 0.35$	430 (393–468)	459 (431–486)	330 (301–359)	$P < 0.001$, G5 < G3, G4	$P = 0.049$, G1 < G4
Bone surface density (mm^{-1})	5.06 (4.80–5.33)	3.55 (3.07–4.03)	$P < 0.001$	4.39 (3.87–4.91)	4.06 (3.83–4.29)	4.33 (3.99–4.66)	$P = 0.39$	$P = 0.005$, G1 > G3
Cortical bone porosity (μm)	405 (376–434)	252 (203–302)	$P < 0.001$	299 (249–349)	326 (287–366)	136 (117–155)	$P < 0.001$, G5 < G3, G4	$P = 0.005$, G1 > G3, G4
Cross sectional area (mm^2)	8.06 (7.69–8.42)	7.83 (7.08–8.57)	$P = 0.64$	8.04 (7.31–8.76)	8.34 (7.47–9.22)	8.00 (7.39–8.62)	$P = 0.62$	$P = 0.67$

Table 6
Summary of collagen and mineral [mean (95% confidence interval)] of subchondral bone tissue (total, medial and lateral)

Groups	2.5-month experimental period			5.5-month experimental period				
	G1: HA	G2: control 2.5	*t* test for G1 and G2	G3: HA-repetition	G4: HA-discontinuation	G5: control 5.5	One-way ANOVA for G3 to G5	One-way ANOVA for all HA groups
Collagen concentration (%)								
Total	20.8 (19.1–22.5)	21.1 (19.6–22.6)	$P = 0.81$	19.0 (18.1–20.0)	19.6 (18.7–20.5)	18.2 (16.9–19.4)	$P = 0.16$	$P = 0.11$
Medial	21.5 (19.4–23.7)	21.3 (18.5–24.1)	$P = 0.92$	19.6 (18.3–20.9)	21.1 (19.6–22.5)	18.6 (17.0–20.3)	$P = 0.053$	$P = 0.17$
Lateral	20.1 (18.2–21.9)	20.8 (19.0–22.6)	$P = 0.54$	18.5 (17.0–20.0)	18.1 (16.7–19.4)	17.7 (16.5–18.9)	$P = 0.71$	$P = 0.18$
Paired *t* test medial vs. lateral	$P = 0.22$	$P = 0.79$		$P = 0.24$	$P = 0.01$	$P = 0.27$		
Mineral concentration (%)								
Total	68.1 (66.9–69.2)	69.1 (68.5–69.8)	$P = 0.14$	67.2 (65.9–68.5)	67.8 (66.5–69.1)	65.1 (63.9–66.2)	$P = 0.01$, G4 > G5	$P = 0.58$
Medial	68.2 (66.8–69.8)	69.1 (68.2–70.1)	$P = 0.36$	67.0 (64.8–69.2)	68.9 (67.4–70.5)	64.9 (63.8–66.0)	$P = 0.008$, G4 > G5	$P = 0.27$
Lateral	67.8 (66.2–69.5)	69.1 (68.0–70.2)	$P = 0.15$	67.4 (65.7–69.0)	66.7 (64.7–68.4)	65.2 (63.3–67.2)	$P = 0.25$	$P = 0.64$
Paired *t* test medial vs. lateral	$P = 0.67$	$P = 0.99$		$P = 0.80$	$P = 0.07$	$P = 0.75$		
Collagen/mineral ratio								
Total	0.25 (0.23–0.27)	0.25 (0.23–0.27)	$P = 0.85$	0.23 (0.22–0.24)	0.24 (0.23–0.24)	0.28 (0.26–0.30)	$P < 0.001$, G5 > G3, G4	$P = 0.22$
Medial	0.22 (0.19–0.24)	0.21 (0.19–0.24)	$P = 0.92$	0.20 (0.18–0.21)	0.21 (0.20–0.23)	0.29 (0.26–0.31)	$P < 0.001$, G5 > G3, G4	$P = 0.12$
Lateral	0.29 (0.27–0.31)	0.31 (0.27–0.34)	$P = 0.49$	0.27 (0.25–0.30)	0.27 (0.25–0.28)	0.27 (0.26–0.29)	$P = 0.88$	$P = 0.16$
Paired *t* test medial vs. lateral	$P < 0.001$	$P = 0.002$		$P < 0.001$	$P < 0.001$	$P = 0.10$		
Tissue density (g/cm^3)								
Total	2.26 (2.25–2.27)	2.28 (2.26–2.30)	$P = 0.15$	2.32 (2.30–0.33)	2.29 (2.28–2.30)	2.15 (2.13–2.17)	$P < 0.001$, G5 < G3, G4	$P < 0.001$, G1 < G3, G4
Medial	2.22 (2.18–2.26)	2.28 (2.26–2.30)	$P = 0.06$	2.30 (2.21–2.39)	2.30 (2.28–2.32)	2.14 (2.11–2.17)	$P < 0.001$, G5 < G3, G4	$P = 0.08$
Lateral	2.29 (2.27–2.30)	2.28 (2.26–2.30)	$P = 0.95$	2.33 (2.28–2.38)	2.27 (2.25–2.29)	2.17 (2.13–2.20)	$P < 0.001$, G5 < G3, G4	$P = 0.044$, G3 > G4
Paired *t* test medial vs. lateral	$P = 0.028$	$P = 0.81$		$P = 0.39$	$P = 0.07$	$P = 0.27$		
Apparent density (g/cm^3)								
Total	0.90 (0.85–0.96)	0.84 (0.78–0.90)	$P = 0.17$	0.94 (0.91–0.97)	0.96 (0.90–1.02)	0.95 (0.91–0.98)	$P = 0.83$	$P = 0.29$
Medial	0.88 (0.85–0.90)	0.85 (0.83–0.88)	$P = 0.21$	0.89 (0.88–0.91)	0.90 (0.87–0.92)	0.81 (0.79–0.82)	$P < 0.001$, G5 < G3, G4	$P = 0.52$
Lateral	0.93 (0.85–1.01)	0.83 (0.74–0.92)	$P = 0.10$	0.99 (0.95–1.04)	1.02 (0.92–1.12)	1.08 (1.02–1.24)	$P = 0.17$	$P = 0.28$
Paired *t* test medial vs. lateral	$P = 0.10$	$P = 0.46$		$P < 0.001$	$P = 0.006$	$P < 0.001$		

ties (Table 7) in the 2.5-month and 5.5-month groups are summarized and the detailed comparisons of the properties between groups are made. There were no significant differences in the properties between the HA repetition and HA discontinuation groups, but there were significant differences in the properties between 2.5-month and 5.5-month HA groups. For the 2.5-month groups, treatment with HA resulted in significantly reduced overall volume fraction of subchondral bone plate. The reduced volume fraction was particularly pronounced in the medial condyle. Moreover, plate thickness and plate surface to volume ratio were significantly lower in the medial condyle of 2.5-month HA group compared with the control group, whereas these parameters were not significantly different in the lateral condyle between the two groups. No significant differences in the properties of subchondral plate in the 5.5-month HA groups compared to the control group were revealed. Both 5.5-month HA groups had greater bone volume fraction and plate thickness compared with the 2.5-month HA group, and changes were particularly pronounced in the medial condyle (Table 3).

Treatment with HA had striking effects on the 3-D microarchitecture of subchondral cancellous bone. In the 2.5-month HA group, cancellous bone had significantly lower bone volume fraction, and greater structure model index compared with the control group. Both 5.5-month HA groups had significantly lower bone volume fraction, connectivity density and bone surface density and greater structure model index and trabecular spacing compared with the control and lower structure model index compared with the 2.5-month HA group (Table 4).

Treatment with HA also had marked effects on the 3-D microarchitecture of subchondral cortical bone. In the 2.5-month HA group, cortical bone had significantly greater bone volume fraction, surface density and mean pore size. Both 5.5-month HA groups had significantly greater bone volume fraction, cortical thickness and mean pore size compared with the control and had greater cortical thickness, surface density and mean pore size compared with the 2.5-month HA group (Table 5).

Treatment with HA had no significant effect on bone collagen and mineral in the 2.5-month HA group whereas both the 5.5-month HA groups had significantly increased bone mineral concentration, mineral density, collagen to mineral ratio and tissue density overall, and in the medial and lateral condyles. Moreover, HA groups also had significantly greater apparent density in the medial condyle in both HA repetition and discontinuation groups. There were no significant differences in the properties for the 2.5-month HA group compared with the 5.5-month HA groups (Table 6).

Treatment with HA neither influenced the mechanical properties of the cancellous bone nor the cortical bone in the 2.5-month HA group and nor the mechanical properties of cancellous bone in the two 5.5-month HA groups. In contrast to cancellous bone, cortical bone showed signifi-

Table 7
Summary of mechanical properties [mean (95% confidence interval)] of subchondral cancellous bone and cortical bone

Groups	2.5-month experimental period			5.5-month experimental period				
	G1: HA	G2: control 2.5	*t* test for G1 and G2	G3: HA-repetition	G4: HA-discontinuation	G5: control 5.5	One-way ANOVA for G3 to G5	One-way ANOVA for all HA groups
Cancellous bone								
Young's modulus (MPa)	289 (232–344)	325 (272–378)	$P = 0.38$	290 (252–329)	296 (246–346)	317 (289–345)	$P = 0.59$	$P = 0.97$
Ultimate stress (MPa)	6.87 (5.21–8.53)	8.33 (6.17–10.5)	$P = 0.32$	8.92 (7.37–10.5)	10.1 (7.77–12.4)	11.3 (9.94–12.7)	$P = 0.31$	$P = 0.07$
Ultimate strain (%)	2.8 (2.5–3.1)	3.1 (2.6–3.6)	$P = 0.31$	3.9 (3.3–4.4)	4.7 (3.4–6.0)	3.8 (3.4–4.2)	$P = 0.14$	$P = 0.02$, G1 < G3, G4
Failure energy (kJ/cm^3)	118 (86–151)	166 (114–219)	$P = 0.16$	195 (149–240)	234 (161–308)	239 (195–282)	$P = 0.43$	$P = 0.019$, G1 < G4
Cortical bone								
Young's modulus (MPa)	2075 (1576–2574)	2584 (2118–3051)	$P = 0.21$	2740 (2211–3270)	2914 (2440–3388)	4104 (3199–5009)	$P = 0.005$, G5 > G3, G4	$P = 0.03$, G1 < G4
Ultimate stress (MPa)	33.6 (27.8–39.3)	39.0 (34.2–43.9)	$P = 0.22$	42.8 (36.6–48.9)	46.1 (41.6–50.7)	42.4 (37.4–47.5)	$P = 0.38$	$P = 0.005$, G1 < G4
Ultimate strain (%)	4.0 (2.4–5.6)	2.7 (2.2–3.2)	$P = 0.23$	3.7 (2.6–4.8)	2.9 (2.3–3.5)	2.0 (1.7–2.3)	$P = 0.003$, G5 < G3	$P = 0.33$
Failure energy (kJ/cm^3)	500 (396–604)	506 (403–610)	$P = 0.56$	677 (567–788)	674 (571–778)	408 (313–503)	$P = 0.002$, G5 < G3, G4	$P = 0.03$

cantly changed mechanical properties with decreased Young's modulus in both 5.5-month HA groups, and increased ultimate strain and failure energy in the 5.5-month HA repetition group. To some extent, the experimental periods were found to significantly influence the mechanical properties of the bone tissues from the HA groups. Thus, the ultimate strain and failure energy of cancellous bone and Young's modulus and ultimate stress of cortical bone showed higher values in one or both the 5.5-month HA groups (Table 7).

Discussion

The present study investigates effects of high molecular weight HA (1.5×10^6 Da) intra-articular injection on the 3-D microarchitecture, mechanical properties, collagen and mineral properties of guinea pig subchondral bone tissues. Our results support the hypothesis that HA effectively protects against cartilage degradation, decreases subchondral bone density and changes its 3-D microstructure such that subchondral bone becomes more compliant (softer). Hence, cartilage stress is reduced during impact loading. The effect of HA was maintained after discontinuation of HA treatment. Thus, there was no significant difference in the properties between the HA repetition and HA discontinuation groups, suggesting that short-term HA treatment (5 weeks) is sufficient to maintain the treatment effects.

Treatment with HA successfully protected against cartilage degeneration. All the HA treated cartilage had almost normal Mankin's score, whereas the control groups had typical OA-related cartilage damage in both the medial and the lateral condyles, and the severity of this degradation progressed from 9 months in the 2.5-month group to 12 months of age in the 5.5-month group, which are consistent with our previous findings [9]. We would like to highlight the fact that early HA treatment protects against cartilage damage. This beneficial effect was maintained without further treatment for the following about 3-month observation period.

Studies in both the human and animal models of OA have demonstrated that the subchondral bone plate is involved in the pathogenesis of OA [7,9]. Enhanced subchondral bone remodeling reflects abnormal bone cell metabolism that may be a strong predictor for OA progression. A clear distinction must be made between the subchondral plate and the underlying cancellous bone [7], since they are two different structures that must be distinguished in their morphology, physiology and mechanical properties [6]. It was shown that increased subchondral plate thickness was associated directly with increased severity of articular cartilage lesions in Cynomolgus Macaques OA, whereas low subchondral plate thickness did not have cartilage lesion [7]. Our current study in guinea pig OA shows a similar result with low subchondral plate thickness that does not lead to cartilage lesion. Although increased subchondral plate thickness was related directly to cartilage damage, there seemed to be an upper limit to the increase of subchondral plate thickness with aging, which did not match the increased severity of cartilage damage in guinea pig OA [9]. Interestingly, both increased and decreased severity of cartilage damage was significantly associated with microarchitectural changes in the underlying subchondral cancellous bone. These results suggest that there are two different mechanisms for the role of subchondral bone contributing to cartilage damages in guinea pig and Cynomolgus Macaques OA models. Treatment with HA for 5 weeks significantly reduced the subchondral plate thickness and volume fraction and protected against cartilage from degradation. It has been observed that significant differences exist between the medial and the lateral condyles of subchondral bone and these differences appeared more frequent in the HA groups.

The most striking effects of HA on subchondral cancellous bone are the pronounced changes in microarchitecture. HA treatment led to significantly lower bone volume fraction with typical rod-like structure. Both 5.5-month HA repetition and discontinuation groups showed more potent effects of HA on cancellous bone microarchitecture that further led to significantly lower connectivity density and surface to volume ratio. The changes in microarchitecture have great significance. Subchondral sclerosis is a typical feature for OA. The increased bone volume fraction and the change to plate-like structure result in high mechanical strength [12]. Therefore, a decreased bone volume fraction and a change to rod-like structure may lead to reduced mechanical strength [12]—e.g. softening of the underlying subchondral bone which may protect cartilage from damage during impact loading.

The significant effects of HA on subchondral cancellous bone and the almost normal Mankin's score of cartilage suggest that subchondral cancellous bone may be involved to a major extent in OA progression. This study is consistent with our previous investigation that covers the entire range of OA from onset to severe stage, and that significant different mechanisms exist in subchondral bone tissues [9]. Monitoring both subchondral bone plate and cancellous bone will help us understand OA initiation and progression. Furthermore, this monitoring may be an indicator of OA progression during intervention and thus provides guidelines for OA therapy.

The current study also showed that treatment with HA for 5 weeks resulted in significantly greater cortical bone volume fraction and surface density. Both repeated and discontinued HA treatments led to significantly greater cortical volume fraction and thickness. The contribution of changes in subchondral cortical shell to OA progression is unclear, but has been considered less important and attracted little attention. In addition, the increased cortical thickness did not lead to greater mechanical properties compared with

the 2.5-month control group, but a lower Young's modulus and greater failure energy in both the 5.5-month HA groups were observed.

Based on investigations in both human and animal OA models, it has been postulated that bone sclerosis can precede cartilage damage and loss [20]. Clinical studies have suggested that there are increases in both bone resorption and formation indices indicating abnormal cellular metabolism due to abnormal osteoblasts characterized by cellular metabolism with increased metabolic activities [22]. The increased metabolic activities in OA bone tissues result in an increased amount of osteoid matrix. The collagen to mineral ratio was significantly higher in the medial condyle than in the lateral condyle. Changes in the subchondral bone may underlie the abnormal bone mineral content, that is, OA bone tissue is sclerotic, yet undermineralized [14,16]. Treatment with HA significantly increases bone mineralization as evidenced by decreased bone collagen to mineral ratio and increased mineral concentration in the subchondral bone tissues. The enhanced bone remodeling in the subchondral bone has been considered the initiating event triggering cartilage damage [20]. Subchondral bone changes may overwhelm the attempts to repair articular cartilage, and failure in cartilage repair may lead to further sclerosis and damage.

There are mainly three primary determinants for cancellous bone strength, i.e. bone matrix density, its microarchitecture and its degree of mineralization [12,15]. Treatment with HA resulted in a significant decreased bone volume fraction and promoted maintenance of a typical rod-like structure. However, these changes did not decrease the mechanical properties in the subchondral cancellous bone, since HA treatment concomitantly increased subchondral bone mineralization as evidenced by a greater bone mineral concentration and a lower bone collagen to mineral ratio. Thus, these findings indicate a cancellous bone quality improvement after HA administration.

Acknowledgments

This study was supported by the Danish Rheumatism Association (Gigtforeningen, Grant no. 233-949-11.07.00), Hørslev-fonden and Helga og Peter Kornings Fond. We thank Jane Pauli, Anette Milton and Eva Mikkelsen for skillful technical assistance, Ulla Dansberg and Hilmar Hald for animal care and Associate Professor Frederik Dagnaes-Hansen for animal experiment advice.

References

[1] Auer JA, Fackelman GE, Gingerich DA, Fetter AW. Effect of hyaluronic acid in naturally occurring and experimentally induced osteoarthritis. Am J Vet Res 1980;41:568–74.
[2] Bendele AM, Hulman JF. Spontaneous cartilage degeneration in guinea pigs. Arthritis Rheum 1988;31:561–5.
[3] Bendele AM, White SL, Hulman JF. Osteoarthrosis in guinea pigs: histopathologic and scanning electron microscopic features. Lab Anim Sci 1989;39:115–21.
[4] Boivin G, Meunier PJ. The mineralization of bone tissue: a forgotten dimension in osteoporosis research. Osteoporos Int 2003; 14(Suppl 3):19–24.
[5] Brown SJ, Pollintine P, Powell DE, Davie MW, Sharp CA. Regional differences in mechanical and material properties of femoral head cancellous bone in health and osteoarthritis. Calcif Tissue Int 2002;71:227–34.
[6] Burr DB. Anatomy and physiology of the mineralized tissues: role in the pathogenesis of osteoarthrosis. Osteoarthr Cartil 2004;12 (Suppl. A):S20–30.
[7] Carlson CS, Loeser RF, Purser CB, Gardin JF, Jerome CP. Osteoarthritis in cynomolgus macaques. III: effects of age, gender, and subchondral bone thickness on the severity of disease. J Bone Miner Res 1996;11:1209–17.
[8] de-Bri E, Reinholt FP, Svensson O. Primary osteoarthrosis in guinea pigs: a stereological study. J Orthop Res 1995;13:769–76.
[9] Ding M, Danielsen CC, Hvid I. Age-related three-dimensional microarchitectural adaptations of subchondral bone tissues in guinea pig primary osteoarthrosis. Submitted 2004.
[10] Ding M, Dalstra M, Danielsen CC, Kabel J, Hvid I, Linde F. Age variations in the properties of human tibial trabecular bone. J Bone Joint Surg Br 1997;79:995–1002.
[11] Ding M, Danielsen CC, Hvid I. Bone density does not reflect mechanical properties in early-stage arthrosis. Acta Orthop Scand 2001;72:181–5.
[12] Ding M, Odgaard A, Danielsen CC, Hvid I. Mutual associations among microstructural, physical and mechanical properties of human cancellous bone. J Bone Joint Surg Br 2002;84:900–7.
[13] Ding M, Odgaard A, Hvid I. Accuracy of cancellous bone volume fraction measured by micro-CT scanning. J Biomech 1999;32: 323–6.
[14] Ding M, Odgaard A, Hvid I. Changes in the three-dimensional microstructure of human tibial cancellous bone in early osteoarthritis. J Bone Joint Surg Br 2003;85:906–12.
[15] Follet H, Boivin G, Rumelhart C, Meunier PJ. The degree of mineralization is a determinant of bone strength: a study on human calcanei. Bone 2004;34:783–9.
[16] Grynpas MD, Alpert B, Katz I, Lieberman I, Pritzker KP. Subchondral bone in osteoarthritis. Calcif Tissue Int 1991;49:20–6.
[17] Hildebrand T, Rüegsegger P. A new method for the model-independent assessment of thickness in three-dimensional images. J Microbiol 1997;185:67–75.
[18] Hogan HA, Ruhmann SP, Sampson HW. The mechanical properties of cancellous bone in the proximal tibia of ovariectomized rats. J Bone Miner Res 2000;15:284–92.
[19] Huebner JL, Otterness IG, Freund EM, Caterson B, Kraus VB. Collagenase 1 and collagenase 3 expression in a guinea pig model of osteoarthritis. Arthritis Rheum 1998;41:877–90.
[20] Lajeunesse D. The role of bone in the treatment of osteoarthritis. Osteoarthr Cartil 2004;12(Suppl. A):S34–8.
[21] Li B, Aspden RM. Mechanical and material properties of the subchondral bone plate from the femoral head of patients with osteoarthritis or osteoporosis. Ann Rheum Dis 1997;56:247–54.
[22] Li B, Marshall D, Roe M, Aspden RM. The electron microscope appearance of the subchondral bone plate in the human femoral head in osteoarthritis and osteoporosis. J Anat 1999;195:101–10.
[23] Mankin HJ, Dorfman H, Lippiello L, Zarins A. Biochemical and metabolic abnormalities in articular cartilage from osteo-arthritic human hips: II. Correlation of morphology with biochemical and metabolic data. J Bone Joint Surg Am 1971;53:523–37.
[24] Mansell JP, Bailey AJ. Abnormal cancellous bone collagen metabolism in osteoarthritis. J Clin Invest 1998;101:1596–603.

[25] Radin EL, Rose RM. Role of subchondral bone in the initiation and progression of cartilage damage. Clin Orthop 1986:34–40.
[26] Uebelhart D, Williams JM. Effects of hyaluronic acid on cartilage degradation. Curr Opin Rheumatol 1999;11:427–35.
[27] Williams JM, Rayan V, Sumner DR, Thonar EJ. The use of intra-articular Na-hyaluronate as a potential chondroprotective device in experimentally induced acute articular cartilage injury and repair in rabbits. J Orthop Res 2003;21:305–11.
[28] Williams JM, Zhang J, Kang H, Ummadi V, Homandberg GA. The effects of hyaluronic acid on fibronectin fragment mediated cartilage chondrolysis in skeletally mature rabbits. Osteoarthr Cartil 2003;11:44–9.